Deep Convolutional Neural Network-Based Detector for Index Modulation

Tengjiao Wang, *Student Member, IEEE*, Fang Yang, *Senior Member, IEEE*, Jian Song, *Fellow, IEEE*, and Zhu Han, *Fellow, IEEE*

***Abstract*—In this letter, a convolutional neural network-based detection framework is proposed for the wireless communication systems using orthogonal frequency-division multiplexing with index modulation (OFDM-IM). In the proposed framework, the received symbols are transformed to polar coordinates to help the neural network detect the indices of the activated subcarriers. We parallel the amplitude and the phase of the received symbols to form 2-dimensional matrices and use 2-dimensional convolutional layers to fully exploit the inherent information in the OFDM-IM symbols. After offline training, the proposed detector can be employed to implement online detection of the OFDM-IM symbols. Simulation results demonstrate that the proposed detector is capable of achieving near maximum likelihood detection performance with much lower complexity.**

***Index Terms*—Convolutional neural network, deep learning, index modulation, polar coordinates, maximum likelihood.**

I. Introduction

In the modern wireless communication systems, orthogonal frequency-division multiplexing (OFDM) has been playing an important role and has been adopted by various communication standards [1]. In OFDM, the entire bandwidth is divided into many narrow-band subcarriers to mitigate inter-symbol interference. OFDM with index modulation (OFDM-IM) is an emerging technique, which allows flexible adjustments of the number of activated subcarriers for a trade-off between error performance and spectral efficiency [2]. In OFDM-IM, only a subset of subcarriers is activated to transmit ordinary amplitude phase modulation (APM) symbols. The information bits are conveyed by not only the ordinary APM symbols, but also the indices of the activated subcarriers [3]. Due to the improved energy efficiency and error performance, OFDM-IM has attracted significant attention and is regarded as a potential candidate for the future wireless communication systems [2].

Deep learning, which utilizes neural networks to extract the inherent features in high-dimensional data, has been used to power many aspects of modern society, such as image recognition, object detection, and natural language processing [4]. In the various deep neural networks, convolutional neural network (CNN) is one particular type, which uses convolutional layers to exploit the local features of the data efficiently [5]. By adopting the convolutional operations, the parameters of the convolutional layers can be shared and the number of parameters can also be greatly reduced. Therefore, CNN has been widely used in many computer vision problems. Recently, the concept of deep learning has been introduced to the physical layer design in wireless communication systems, including channel modeling, decoding, and signal detection [6].

In the literatures, many signal detection methods have been proposed for the OFDM-IM systems. In [7], a log-likelihood ratio (LLR) detector is proposed for OFDM-IM to achieve near-optimal detection performance. A low-complexity detector based on the maximum-likelihood (ML) criterion is proposed and analyzed in [8]. In recent research works, several deep learning-based signal detection methods have been proposed for the OFDM and OFDM-IM systems. In [9], a deep learning-based channel estimation and signal detection method is proposed for OFDM systems, which employs a neural network consisting of five fully connected (FC) layers to detect the OFDM signals. In [10], the authors use traditional communication solutions as initializations for the neural network to further improve detection accuracy. The research works presented in [11] focus on signal detection of OFDM-IM systems. A deep neural network (DNN) consisting of two FC layers is adopted to detect the OFDM-IM symbols. However, only the FC layers are taken into consideration in these methods [9]–[11], which involve a large number of parameters to be optimized and limit the detection performance.

In this letter, a CNN-based detection framework is proposed for the OFDM-IM systems, which is termed as CNN-IM. In the proposed CNN-IM framework, the convolutional layers and pre-processing procedure are adopted to detect the OFDM-IM symbols efficiently. The contributions of this letter can be summarized as follows.

- Different from the state-of-the-art deep learning-based methods [9]–[11], which concatenate the real part and imaginary part of the received symbols to form 1-dimensional input vectors, we arrange the received symbols as 2-dimensional input matrices and use a 2-dimensional convolutional layer to fully exploit the inherent information in the OFDM-IM symbols.
- We utilize a pre-processing procedure in the CNN-IM detector to transform the OFDM-IM symbols to polar co-

This work was partially supported by National Natural Science Foundation of China under Grant 61871255, Natural Science Foundation of Guangdong Province under Grant 2015A030312006, National Key Research and Development Program of China under Grant 2017YFE0113300, US Multidisciplinary University Research Initiative 18RT0073, NSF EARS-1839818, CNS-1717454, and CNS-1731424. *(Corresponding author: Fang Yang.)*

Tengjiao Wang, Fang Yang, and Jian Song are with the Department of Electronic Engineering, Beijing National Research Center for Information Science and Technology, Tsinghua University, Beijing 100084, China, and also with the Key Laboratory of Digital TV System of Guangdong Province and Shenzhen City, Research Institute of Tsinghua University in Shenzhen, Shenzhen 518057, China (e-mail: wangtj16@mails.tsinghua.edu.cn; fangyang@tsinghua.edu.cn; jsong@tsinghua.edu.cn).

Zhu Han is with the University of Houston, Houston, TX 77004 USA, and also with the Department of Computer Science and Engineering, Kyung Hee University, Seoul, South Korea, 446-701 (e-mail: zhan2@uh.edu).

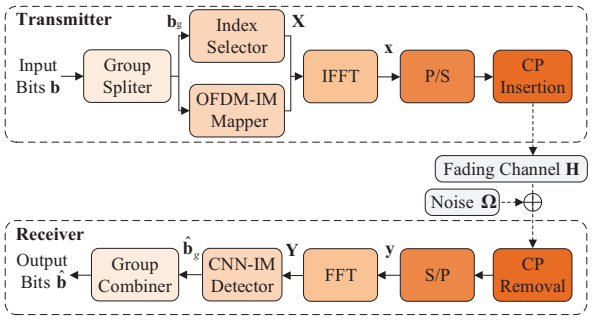


Fig. 1. Block diagram of the OFDM-IM communication system.

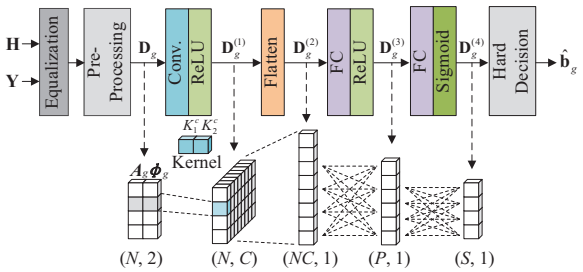


Fig. 2. Framework of the proposed CNN-IM detector.

ordinates to help the neural network detect the indices of the activated subcarriers and improve detection accuracy.
- The performance of the proposed CNN-IM detector is evaluated through computer simulations. The results valid that the proposed CNN-IM detector is capable of achieving near-ML detection performance with much lower complexity under both perfect and imperfect channel estimations.

The rest of the letter is organized as follows. In Section II, the system model of the communication system using OFDM-IM is illustrated. The details of the proposed CNN-IM detector are presented in Section III, including the framework, the offline training procedure, and the online deployment. In Section IV, simulation results and corresponding discussions are provided. Finally, this letter is concluded in Section V.

II. System Model

We consider a wireless communication system using OFDM-IM. The entire bandwidth is divided into N_f subcarriers. The subcarriers are further split into G groups, each of which contains $N = N_\mathrm{f}/G$ subcarriers. According to the principle of OFDM-IM [2], only N_a subcarriers are activated to transmit the M-level APM symbols in each subcarrier group, and the other $(N - N_\mathrm{a})$ subcarriers are zero padded. Therefore, $S_1 = N_\mathrm{a}\log_2(M)$ bits can be transmitted through the APM symbols and $S_2 = \lfloor \log_2 \binom{N}{N_\mathrm{a}} \rfloor$ bits can be conveyed by the indices of the activated subcarriers in each subcarrier group, where $\binom{\cdot}{\cdot}$ denotes the binomial coefficient. As a result, $S = S_1 + S_2$ bits can be conveyed by each subcarrier group and GS bits can be conveyed by the whole OFDM-IM symbol.

The block diagram of the system is shown in Fig. 1. At the transmitter, the input bits $\mathbf{b} \in \mathbb{B}^{GS\times 1}$ are split into G blocks $\mathbf{b}_g \in \mathbb{B}^{S\times 1}$ $(g = 1, 2, \cdots, G)$ to direct the index selector and the OFDM-IM mapper in each subcarrier group. Then the generated frequency-domain symbol $\mathbf{X} \in \mathbb{C}^{N_\mathrm{f}\times 1}$ is fed into the N_f-point inverse fast Fourier transform (IFFT) module to derive the time-domain symbol $\mathbf{x} \in \mathbb{C}^{N_\mathrm{f}\times 1}$. After parallel-to-serial (P/S) conversion and cyclic prefix (CP) insertion, the time-domain symbols are transmitted through the wireless channel. At the receiver, after CP removal and serial-to-parallel (S/P) conversion, the received time-domain symbol $\mathbf{y} \in \mathbb{C}^{N_\mathrm{f}\times 1}$ is fed into the N_f-point fast Fourier transform (FFT) module to derive the frequency-domain symbol $\mathbf{Y} \in \mathbb{C}^{N_\mathrm{f}\times 1}$. Then the proposed CNN-IM detector is utilized to recover the information bits $\hat{\mathbf{b}}_g \in \mathbb{B}^{S\times 1}$ in each subcarrier group from $\mathbf{Y}$. Finally, they are combined as the estimated information bits $\hat{\mathbf{b}} \in \mathbb{B}^{GS\times 1}$. The frequency-domain transmission function can be given as

$$\mathbf{Y} = \mathbf{H} \otimes \mathbf{X} + \mathbf{\Omega}, \tag{1}$$

where $\mathbf{H} \in \mathbb{C}^{N_\mathrm{f}\times 1}$ denotes the Rayleigh fading channel coefficient, the element of which follows $H_n \sim \mathcal{CN}(0, 1)$ $(n = 1, 2, \cdots, N_\mathrm{f})$. $\mathbf{\Omega} \in \mathbb{C}^{N_\mathrm{f}\times 1}$ denotes the additive white Gaussian noise (AWGN), the element of which follows $\Omega_n \sim \mathcal{CN}(0, \sigma^2)$. $\otimes$ represents the element-wise multiplication.

III. Proposed CNN-IM Detector

In this section, the framework of the proposed CNN-IM detector is introduced in Section III-A. The corresponding offline training procedure and the online deployment are explained in Section III-B.

A. Framework of the CNN-IM Detector

The proposed CNN-IM detector consists of several modules and neural network layers, including one equalization module, one pre-processing module, one convolutional (Conv.) layer, one flatten layer, two FC layers, and one hard decision module. The functions and parameters of these modules and layers are explained in the following paragraphs. An illustration of the framework is given in Fig. 2.

Equalization: The equalization module is used to combat the frequency-selective channel fading, which is supposed to be known at the receiver. In this letter, we adopt the simplest zero-forcing (ZF) equalization method. The symbols after equalization can be given as

$$\hat{\mathbf{X}} = \mathbf{H}^{-1} \otimes \mathbf{Y} = \mathbf{X} + \mathbf{H}^{-1} \otimes \mathbf{\Omega}. \tag{2}$$

Pre-Processing: Firstly, we split the symbols $\hat{\mathbf{X}} \in \mathbb{C}^{N_\mathrm{f}\times 1}$ into G blocks $\hat{\mathbf{X}}_g \in \mathbb{C}^{N\times 1}$ for decoding the information in each subcarrier group. Then, the complex symbols $\hat{\mathbf{X}}_g$ need to be transformed before they are fed into the following neural network layers, which only take in real numbers [4]. Different from the state-of-the-art deep learning-based methods [9]–[11], which separate the real part and imaginary part of the complex symbols as the inputs for neural networks, here, we handle the received complex symbols based on polar instead of Cartesian coordinate representations. Specifically, we utilize

the amplitude $\boldsymbol{A}_g \in \mathbb{R}^{N\times 1}$ and phase $\boldsymbol{\phi}_g \in \mathbb{R}^{N\times 1}$ of the symbols $\hat{\mathbf{X}}_g$ as the inputs for the neural networks in order to help the network detect the indices of the activated subcarriers. This is based on the consideration that the activated subcarrier and the non-activated subcarrier differ a lot in symbol amplitude when using OFDM-IM. Moreover, different from the state-of-the-art deep learning-based methods [9]–[11], which concatenate the real part and imaginary part of the symbols to form 1-dimensional vectors, we parallel the amplitude and the phase to form 2-dimensional matrices $\mathbf{D}_g = [\mathbf{A}_g, \boldsymbol{\phi}_g] \in \mathbb{R}^{N\times 2}$ in order to fully exploit the inherent information between them.

Conv. Layer: Then, the matrices $\mathbf{D}_g$ is fed into a 2-dimensional Conv. layer with convolutional kernel $\mathbf{K}^c = [K_1^c, K_2^c] \in \mathbb{R}^{1\times 2}$ $(c = 1, 2, \cdots, C)$ of C output channels to exploit the features in $\mathbf{D}_g$. The widely used rectified linear unit (ReLU) function $f_{\text{ReLU}}(x) = \max(0, x)$ is utilized as the activation function of the Conv. layer. We denote the output of the Conv. layer as $\mathbf{D}_g^{(1)} \in \mathbb{R}^{N\times C}$, which can be derived as

$$\mathbf{D}_g^{(1)}[n, c] = f_{\text{ReLU}}\left(\sum_{i=1}^{2} \mathbf{D}_g[n, i] \times K_i^c + B^c\right), \tag{3}$$

where $\mathbf{D}_g^{(1)}[n, c]$ denotes the element at the n-th row and the c-th column of $\mathbf{D}_g^{(1)}$. $\mathbf{D}_g[n, i]$ denotes the element at the n-th row and the i-th column of $\mathbf{D}_g$. B^c denotes the bias for the c-th output channel.

Flatten Layer: A flatten layer succeeds the Conv. layer to transform the 2-dimensional matrix $\mathbf{D}_g^{(1)}$ into a 1-dimensional vector $\mathbf{D}_g^{(2)} \in \mathbb{R}^{NC\times 1}$.

FC Layers: After flatten, vector $\mathbf{D}_g^{(2)}$ is fed into two FC layers. For the first FC layer, the ReLU activation function is adopted. We denote the weights and biases of the first FC layer as $\mathbf{W}_1 \in \mathbb{R}^{P\times NC}$ and $\mathbf{b}_1 \in \mathbb{R}^{P\times 1}$. The output vector $\mathbf{D}_g^{(3)} \in \mathbb{R}^{P\times 1}$ of the first FC layer can be expressed as

$$\mathbf{D}_g^{(3)} = f_{\text{ReLU}}\left(\mathbf{W}_1 \times \mathbf{D}_g^{(2)} + \mathbf{b}_1\right). \tag{4}$$

For the second FC layer, the Sigmoid activation function $f_{\text{Sigmoid}}(x) = 1/(1 + e^{-x})$ is adopted to map the elements of the output vector to the interval $(0, 1)$. Therefore, the output vector $\mathbf{D}_g^{(4)} \in \mathbb{R}^{S\times 1}$ of the second FC layer can be expressed as

$$\mathbf{D}_g^{(4)} = f_{\text{Sigmoid}}\left(\mathbf{W}_2 \times \mathbf{D}_g^{(3)} + \mathbf{b}_2\right), \tag{5}$$

where $\mathbf{W}_2 \in \mathbb{R}^{S\times P}$ and $\mathbf{b}_2 \in \mathbb{R}^{S\times 1}$ denote the weights and biases of the second FC layer, respectively.

Hard Decision: Finally, the estimated information bits $\hat{\mathbf{b}}_g$ can be derived by the hard decision decoding, which can be expressed as

$$\hat{\mathbf{b}}_g[s] = \begin{cases} 1, & \mathbf{D}_g^{(4)}[s] \geq 0.5, \\ 0, & \mathbf{D}_g^{(4)}[s] < 0.5, \end{cases} \tag{6}$$

where $\hat{\mathbf{b}}_g[s]$ and $\mathbf{D}_g^{(4)}[s]$ $(s = 1, 2, \cdots, S)$ denote the s-th element of vector $\hat{\mathbf{b}}_g$ and $\mathbf{D}_g^{(4)}$, respectively.

B. Offline Training and Online Deployment

The proposed CNN-IM detector needs to be trained offline before online deployment. The training information bits are randomly generated and they are processed according to the system model described in Section II. The training channel coefficient and the noise are randomly generated based on their statistic models, which are independently generated for each OFDM-IM symbol. The parameters of the CNN-IM detector can be summarized as

$$\boldsymbol{\theta} = \{\mathbf{K}^1, \cdots, \mathbf{K}^C, B^1, \cdots, B^C, \mathbf{W}_1, \mathbf{b}_1, \mathbf{W}_2, \mathbf{b}_2\}. \tag{7}$$

These parameters are optimized in the offline training procedure. In this letter, we adopt the mean-squared error (MSE) loss function to measure the difference between the estimated bits and the real training bits, which can be expressed as

$$\mathcal{L}(\mathbf{b}_g, \hat{\mathbf{b}}_g) = \frac{1}{S}\|\mathbf{b}_g - \hat{\mathbf{b}}_g\|^2. \tag{8}$$

Then, the parameters $\boldsymbol{\theta}$ can be optimized through lots of sophisticated optimizers, including the stochastic gradient descent (SGD) optimizer, the adaptive moment estimation (Adam) optimizer, and so on.

After offline training, the CNN-IM detector with the optimal parameters $\boldsymbol{\theta}^*$ can be employed at the receiver to provide real-time detection for the received symbols. Once the received frequency-domain symbols $\mathbf{Y}$ and the channel coefficient $\mathbf{H}$ are fed into the CNN-IM detector, it can estimate the information bits $\hat{\mathbf{b}}_g$ immediately according to the framework described in Section III-A.

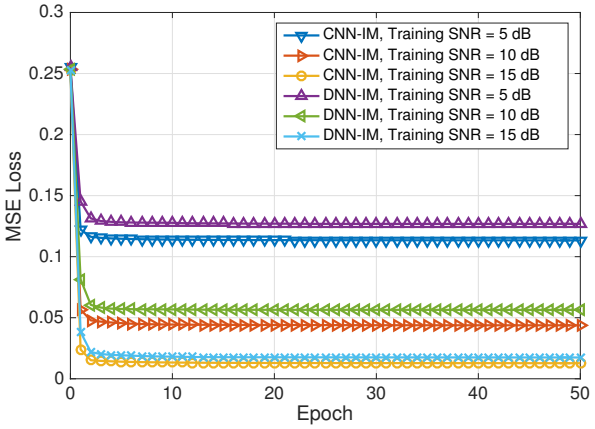


Fig. 3. Comparisons of the MSE loss of the proposed CNN-IM detector and DNN-based detector with different training SNRs.

IV. Simulation Results

In this section, the MSE loss, bit error rate (BER), and the computational complexity of the proposed CNN-IM detector are analyzed, respectively. We consider a an OFDM-IM system with $N_{\text{f}} = 64$ subcarriers. The subcarriers are further split into $G = 16$ groups with $N = N_{\text{f}}/G = 4$ subcarriers in each group. 4QAM modulation is adopted and $N_a = 3$ subcarriers are activated in each subcarrier group. The proposed CNN-IM detector is implemented on the PyTorch platform [12]. The hyper-parameters for the neural layers are set to be $C = 16$ and $P = 50$. In the offline training procedure, the widely used Adam optimizer is adopted with learning rate $\eta = 0.005$. Mini-batch is utilized to accelerate the training procedure with $B =$

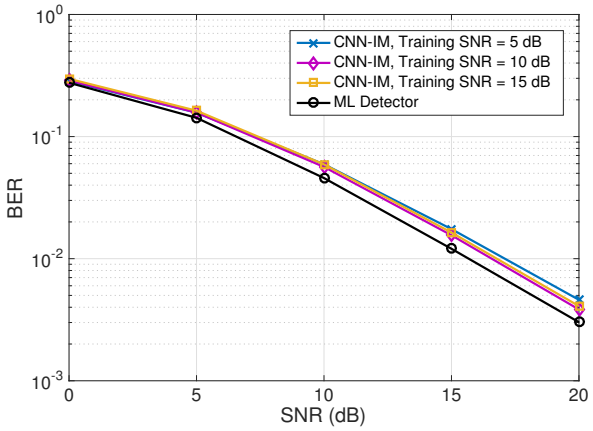


Fig. 4. Comparisons of the BER performance of the proposed CNN-IM detectors with different training SNRs.

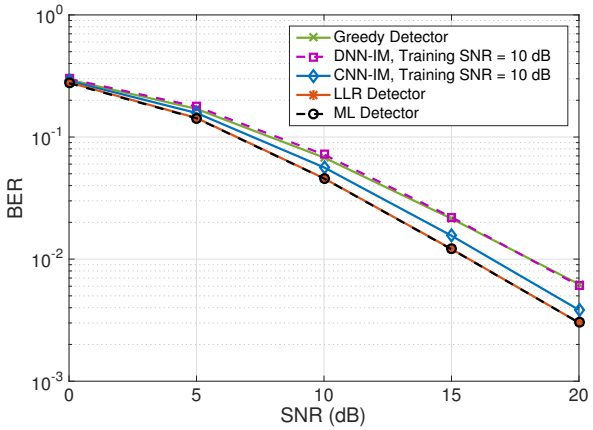


Fig. 5. Comparisons of the BER performance of the proposed CNN-IM detector with the state-of-the-art detectors.

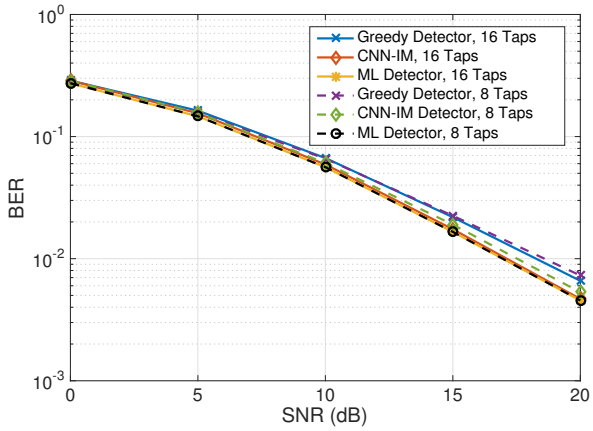


Fig. 6. Comparisons of the BER performance of the proposed CNN-IM detector under correlated frequency-selective channels.

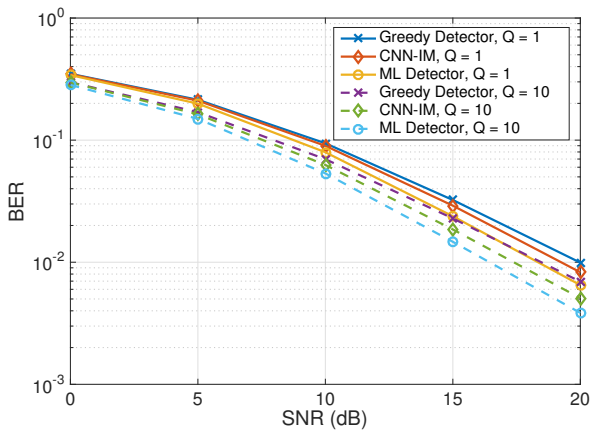


Fig. 7. Comparisons of the BER performance of the proposed CNN-IM detector with channel estimation errors.

64 OFDM-IM symbols in each mini-batch. The training data set and the testing data set contain 1.6×10^5 and 1.0×10^4 randomly generated OFDM-IM symbols, respectively.

A. MSE Loss Analyses

We first analyze the MSE loss of the proposed CNN-IM detector in the offline training procedure. The conventional DNN-based detector is also simulated for comparison. The DNN-based detector contains two FC layers, which have the same number of neurons as the proposed CNN-IM detector $P = 50$. The MSE loss with different training signal to noise ratios (SNRs) are illustrated in Fig. 3. It can be seen that the CNN-IM detector trained with a higher SNR has much lower MSE loss. For all the simulated circumstances, the proposed CNN-IM detector exhibits lower MSE than the DNN-based detector. It shows the CNN-IM detector can provide satisfactory detection performance within 50-epoch training, which ensures the fast deployment of the detector.

B. BER Analyses

Firstly, we investigate the BER performance of the proposed CNN-IM detector with different training SNRs. The group-wise ML detector is also simulated for comparison. The Rayleigh fading channel defined in Section II is considered. After trained offline for 50 epochs, the CNN-IM detector is deployed online to detect the symbols in the test data set. The simulation results are shown in Fig. 4. It can be seen that the proposed CNN-IM detector exhibits slightly different BERs under different training SNRs. The CNN-IM detector trained at SNR of 10 dB exhibits the best BER performance, only 1.2 dB worse than the ML detector at SNR of 20 dB.

Then, we compare the BER performance of the proposed CNN-IM detector with state-of-the-art detectors under Rayleigh fading channel conditions. The LLR detector [7], the DNN-based detector [11], and the conventional greedy detector [13] are also simulated for comparison. The CNN-IM detector and the DNN-based detector are trained at SNR of 10 dB for 50 epochs. As shown in Fig. 5, the BERs of all the detectors decrease with the increase of the SNRs. The greedy detector and the DNN-based detector achieve the worst BER performance in the entire simulated SNR region. The proposed CNN-IM detector has much better BER performance than the DNN-based detector, which is mainly because that the pre-processing and the convolutional layer can

TABLE I
COMPARISONS OF THE COMPUTATIONAL COMPLEXITY

Methods	Complexity (flops)
CNN-IM	$2PCGN + 5CGN + 2SPG + 12GN + PG + 3SG$
ML	$\binom{N}{N_a} \times M^{N_a} \times (12GN)$
LLR	$14MGN + \alpha MGN + GN^2 + (\alpha+\beta+6)GN + 12MGN_a^{\dagger}$
DNN-IM	$4PGN + 2SPG + 6GN + PG + 3SG$

† Here, α and β denote the number of flops required for the $\exp(\cdot)$ function and the $\ln(\cdot)$ functions, respectively.

help the neural network exploit the inherent information in the OFDM-IM symbols. The LLR detector can achieve better BER performance than the proposed CNN-IM detector. However, when using LLR detector, the variance of the AWGN noise needs to be perfectly known at the receiver.

Finally, we investigate the BER performance of the CNN-IM detector under realistic channel conditions [14]. In Fig. 6, the correlated frequency-selective channel defined in [7] is considered, where the channel impulse response is defined as $\mathbf{h} = [h_1, h_2, \cdots, h_L]$, where L denotes the number of channel taps, and each element follows $h_l \sim \mathcal{CN}(0, 1/L)$ ($l = 1, 2, \cdots, L$). The CNN-IM detector is trained under the Rayleigh fading channel for 50 epochs, and is used to detect the signals under the correlated frequency-selective channels with 8 taps and 16 taps. It can be seen from Fig. 6 that the proposed CNN-IM detector can achieve near-ML BER performance under both channel conditions, which shows that the proposed CNN-IM detector can serve as a promising detector for the frequency-selective channels with different number of channel taps. We also analyze the BER performance with channel estimation errors. As defined in [7], the estimated channel is given by $\tilde{\mathbf{H}} = \mathbf{H} + \boldsymbol{\epsilon}$, where the estimation errors follow $\boldsymbol{\epsilon} \sim \mathcal{CN}(\mathbf{0}, \sigma_\epsilon^2 \mathbf{I}_{N_t})$. The AWGN noise and the channel estimation errors are related via $Q = \sigma^2/\sigma_\epsilon^2$. The simulation results are provided in Fig. 7 with $Q = 1$ and $Q = 10$. The CNN-IM detector is trained under the Rayleigh fading channel for 50 epochs. It can be seen that the proposed CNN-IM detector exhibits better BER performance than the greedy detector in both scenarios.

C. Complexity Analyses

In the end, we analyze the complexity of the CNN-IM detector in the online detecting phase. The total number of real floating-point operations (flops) are measured, including addition, subtraction, multiplication, division, and other operations for real numbers [15]. For each OFDM-IM symbol, the equalization takes $(6GN)$ flops. The pre-processing procedure takes $(6GN)$ flops for transforming the symbols to polar coordinates. The Conv. layer and ReLU function contain $(5CGN)$ flops. The first and second FC layers with corresponding activation functions contain $(2PCGN + PG)$ and $(2SPG + 3SG)$ flops, respectively. The total complexity is summarized in Table I and the complexity of the group-wise ML detector is also provided as a comparison. For example, when 16QAM is adopted, the group-wise ML detector needs about 1.3×10^7 flops, and the proposed CNN-IM only needs 1.2×10^5 flops. It validates that the proposed CNN-IM detector can reduce the complexity greatly.

V. CONCLUSION

This letter presents our attempt to build a CNN-based detection framework for the wireless communication systems using OFDM-IM. The 2-dimensional convolutional layer is adopted to extract the features in the OFDM-IM symbols efficiently. Based on the structure of the OFDM-IM symbols, pre-processing is conducted to improve the detection accuracy. Simulations validate that the proposed CNN-IM detector can achieve near-ML detection performance with greatly reduced complexity. The proposed framework using 2-dimensional convolutional layers can serve as a promising candidate for the signal detections in the future communication systems.

REFERENCES

[1] T. Hwang, C. Yang, G. Wu, S. Li, and G. Ye Li, "OFDM and its wireless applications: A survey," *IEEE Trans. Veh. Technol.*, vol. 58, no. 4, pp. 1673–1694, May 2009.

[2] E. Basar, M. Wen, R. Mesleh, M. Di Renzo, Y. Xiao, and H. Haas, "Index modulation techniques for next-generation wireless networks," *IEEE Access*, vol. 5, pp. 16 693–16 746, Aug. 2017.

[3] T. Wang, F. Yang, C. Pan, L. Cheng, and J. Song, "Spectral-efficient hybrid dimming scheme for indoor visible light communication: A subcarrier index modulation based approach," *J. Lightw. Technol.*, vol. 37, no. 23, pp. 5756–5765, Dec. 2019.

[4] Y. LeCun, Y. Bengio, and G. Hinton, "Deep learning," *Nature*, vol. 521, pp. 436–44, May 2015.

[5] A. Krizhevsky, I. Sutskever, and G. E. Hinton, "ImageNet classification with deep convolutional neural networks," in *Neural Information Processing Systems (NIPS)*, Lake Tahoe, NV, Dec. 2012, pp. 1097–1105.

[6] T. O'Shea and J. Hoydis, "An introduction to deep learning for the physical layer," *IEEE Trans. on Cogn. Commun. Netw.*, vol. 3, no. 4, pp. 563–575, Dec. 2017.

[7] E. Basar, U. Aygolu, E. Panayirci, and H. V. Poor, "Orthogonal frequency division multiplexing with index modulation," *IEEE Trans. Signal Process.*, vol. 61, no. 22, pp. 5536–5549, Nov. 2013.

[8] B. Zheng, F. Chen, M. Wen, F. Ji, H. Yu, and Y. Liu, "Low-complexity ML detector and performance analysis for OFDM with in-phase/quadrature index modulation," *IEEE Commun. Lett.*, vol. 19, no. 11, pp. 1893–1896, Nov. 2015.

[9] H. Ye, G. Y. Li, and B. Juang, "Power of deep learning for channel estimation and signal detection in OFDM systems," *IEEE Wireless Commun. Lett.*, vol. 7, no. 1, pp. 114–117, Feb. 2018.

[10] X. Gao, S. Jin, C. Wen, and G. Y. Li, "ComNet: Combination of deep learning and expert knowledge in OFDM receivers," *IEEE Commun. Lett.*, vol. 22, no. 12, pp. 2627–2630, Dec. 2018.

[11] T. V. Luong, Y. Ko, N. A. Vien, D. H. N. Nguyen, and M. Matthaiou, "Deep learning-based detector for OFDM-IM," *IEEE Wireless Commun. Lett.*, vol. 8, no. 4, pp. 1159–1162, Aug. 2019.

[12] A. Paszke, S. Gross, S. Chintala, G. Chanan, E. Yang, Z. DeVito, Z. Lin, A. Desmaison, L. Antiga, and A. Lerer, "Automatic differentiation in PyTorch," in *Neural Information Processing Systems (NIPS)*, Long Beach, CA, Dec. 2017.

[13] J. Crawford and Y. Ko, "Low complexity greedy detection method with generalized multicarrier index keying OFDM," in *IEEE 26th Annual International Symposium on Personal, Indoor, and Mobile Radio Communications (PIMRC)*, Hong Kong, China, Aug. 2015, pp. 688–693.

[14] Q. Shi, N. Wu, H. Wang, and W. Yuan, "Joint channel estimation and decoding in the presence of phase noise over time-selective flat-fading channels," *IET Commun.*, vol. 10, no. 5, pp. 577–585, Dec. 2016.

[15] T. Wang, S. Liu, F. Yang, J. Wang, J. Song, and Z. Han, "Generalized spatial modulation-based multi-user and signal detection scheme for terrestrial return channel with NOMA," *IEEE Trans. Broadcast.*, vol. 64, no. 2, pp. 211–219, Jun. 2018.